Stepwise Functionalization-Induced Molecular Tweak Unveiling Multi-Level Thermochromic Data Encryption and Fingerprint Monitoring System

Debika Barman, [a] Retwik Parui, [a] Parameswar Krishnan Iyer* [a,b]

[a] Department of Chemistry, Indian Institute of Technology Guwahati, Guwahati-781039, India

[b] Centre for Nanotechnology, Indian Institute of Technology Guwahati, Guwahati-781039, India

Experimental Section

Materials

Thianthrene, malonitrile, 4-Bromobenzoylchloride, 3-Bromobenzoylchloride, 2-Bromobenzoylchloride, 4-Pyridinylboronic acid, Aluminium chloride, Tetrakis(triphenylphosphine)palladium(0), potassium carbonate, Titanium chloride, piperidine and methyliodide were purchased from Sigma-Aldrich and used without any further purification. All the solvents like DCM, DMF, THF, Toluene, Ethanol, Chloroform and Hexane were purchased and purified before using following standard protocols and stored in molecular sieves.

Optical Characterization

The absorption and fluorescence spectra were measured using a PerkinElmer instrument, a Horiba-Fluoromax4 paired with a Varian Cary Eclipse spectrometer, and a Model Lambda-25 spectrometer, respectively. Time-resolved photoluminescence lifetimes were determined through time-resolved studies conducted with the Edinburgh FLS 1000 instrument. All quantum yield and steady-state photoluminescence measurements of the isomers in the aggregated state were performed in water (50 μM) using a 405 nm excitation source. Solid-state measurements were carried out using a 430 nm excitation wavelength. Fluorescence lifetime measurements for both aggregated and solid-state samples were conducted using a 405 nm pulsed laser excitation source.

Morphology Visualization

The morphology of the nanoaggregates was analyzed using field emission scanning electron microscopy (FESEM) with a Zeiss Sigma-300 model.

XRD Data

Powder X-ray diffraction (PXRD) measurements of the sample were performed using a Rigaku SmartLab X-ray diffractometer, employing a copper Kα source (λ = 1.54 Å) with a 9 kW power output. The single-crystal X-ray diffraction (SCXRD) structures of *p*-TPy, and *m*-TPy were obtained using X-ray diffractometers from Bruker. The Bruker diffractometer featured a Mo Kα X-ray source (Mova), a CCD detector (Eos), Autochem software, Crystal AlisPRO software, and an Oxford cryo system (operating between 80−500 K). All self-assembled and co-assembled crystal structures were solved and refined using SHELXL2018, and SHELXL2019, employing direct methods and the least-squares method, respectively.

Computational Studies

To examine the influence of positional isomerism on electronic distribution and the variation in HOMO–LUMO band gaps, the electronic properties of all three isomers (*p*-TPy, *m*-TPy, and *o*-TPy) were theoretically investigated using density functional theory (DFT). The ground-state geometries of the compounds were optimized employing the B3LYP functional with the 6-31G basis set as implemented in the Gaussian 09 software package. Along with the calculation of HOMO–LUMO energy gaps, dihedral angles were extracted from the optimized structures to gain deeper insight into the molecular conformations and degrees of twist within the molecules.

Preparation of TLMs

Thermochromic luminescent material (TLM) inks with distinct thermochromic transition temperatures were prepared by blending the *para*-isomer, *p*-TPy, with chloroform and different molecular weight polyethylene glycols (PEG2000, PEG4000, and PEG20000), resulting in ink formulations A, B, C, and D, respectively. These inks were subsequently used for writing letters, numbers, and binary codes. Ink A was prepared by dissolving 2 mg of *p*-TPy in 100 μL of chloroform without the addition of PEG. For inks B, C, and D, 2 mg of *p*-TPy was dissolved in 100 μL of chloroform, followed by the addition of 30 mg of PEG2000, PEG4000, or PEG20000, respectively. The resulting homogeneous solution was then coated onto a clean glass slide. Under 375

nm UV irradiation, the TLM ink-coated slide exhibited a characteristic red luminescence.

Development of LFP by soaking method

To reduce interference from latent fingerprint (LFP) residue components, volunteers were instructed to gently wipe their foreheads with their fingertips before pressing their fingers onto designated substrate surfaces to deposit LFPs. The resulting LFPs were then treated by dipping into the aqueous *p*-TPyMe solution (50 μM) directly onto the substrate, ensuring complete coverage. After allowing the solution to interact with the LFPs for 1 minute, the excess liquid was carefully removed without any additional processing. The developed fingerprints were subsequently imaged under 365 nm UV illumination using a DSLR camera.

Synthetic Procedure

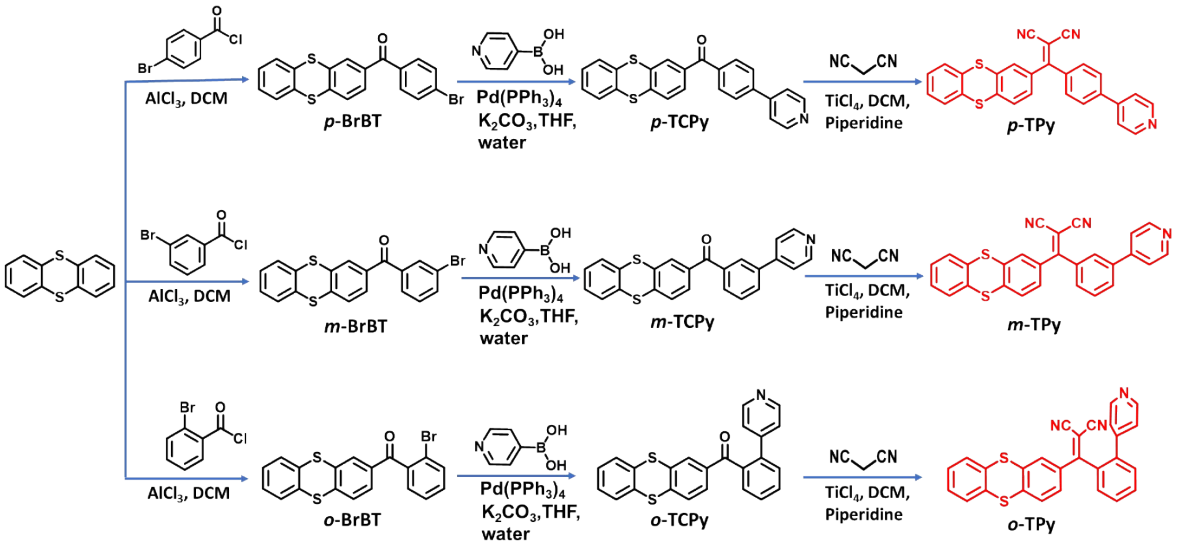

Scheme 1. Synthetic route of the positional isomers, *p*-TPy, *m*-TPy and *o*-TPy.

Synthesis of (4-bromophenyl)(thianthren-2-yl)methanone (p-BrBT/m-BrBT/o-BrBT):

Anhydrous $AlCl_3$ (368 mg, 2.76 mmol) in DCM is slowly added to benzoyl chloride (510 mg, 2.76 mmol) in a 100 mL round-bottom flask (RB) at 0 °C. Thianthrene (500 mg, 2.3 mmol) is

then dissolved in DCM and added dropwise to the reaction mixture. The mixture is allowed to warm to room temperature (RT) and stirred for 24 hours. After completion, extract the product using DCM and a brine solution. The product is purified by column chromatography using a 20% chloroform/hexane mixture, yielding 850 mg of a light yellow solid (91% yield). ^{1}H NMR (600 MHz, $CDCl_3$) δ 7.83 (s, 1H), 7.61 (d, *J* = 6.2 Hz, 4H), 7.54 (d, *J* = 8.0 Hz, 1H), 7.46 (s, 0H), 7.27 – 7.23 (m, 1H). ^{13}C NMR (151 MHz, $CDCl_3$) δ 194.32, 141.60, 136.72, 136.16, 136.11, 134.78, 134.51, 131.99, 131.61, 130.01, 129.26, 129.09, 128.97, 128.62, 128.38, 128.31, 128.03.

Similarly *m*-BrBT was synthesized following same procedure as *p*-BrBT and light yellow product is obtained with 88.69 % yield (820 mg). ^{1}H NMR (600 MHz, $CDCl_3$) δ 7.87 (d, *J* = 1.8 Hz, 1H), 7.65 (ddd, *J* = 8.1, 2.9, 1.5 Hz, 2H), 7.54 (d, *J* = 8.1 Hz, 1H), 7.48 – 7.45 (m, 2H), 7.43 (td, *J* = 7.5, 1.2 Hz, 1H), 7.37 (td, *J* = 7.7, 1.8 Hz, 1H), 7.31 (dd, *J* = 7.4, 1.8 Hz, 1H), 7.28 – 7.25 (m, 3H). ^{13}C NMR (151 MHz, $CDCl_3$) δ 194.48, 142.72, 140.17, 136.10, 135.60, 134.53, 134.18, 133.31, 131.42, 129.86, 129.27, 128.94, 128.86, 128.72, 128.61, 128.19, 128.09, 127.36, 119.49.

Similarly *o*-BrBT was synthesized following same procedure as *p*-BrBT and light yellow product is obtained with 85.12 % yield (790 mg). ^{1}H NMR (600 MHz, $CDCl_3$) δ 7.94 – 7.88 (m, 2H), 7.75 (ddd, *J* = 8.0, 2.0, 1.0 Hz, 1H), 7.71 – 7.64 (m, 2H), 7.60 (d, *J* = 8.0 Hz, 1H), 7.51 (ddd, *J* = 5.6, 3.3, 1.1 Hz, 2H), 7.39 (t, *J* = 7.8 Hz, 1H), 7.30 (dd, *J* = 5.8, 3.3 Hz, 2H). ^{13}C NMR (151 MHz, $CDCl_3$) δ 193.72, 141.67, 139.13, 136.32, 136.11, 135.53, 134.60, 134.30, 132.63, 130.00, 129.83, 129.13, 128.91, 128.78, 128.44, 128.38, 128.20, 128.12, 122.79.

Synthesis of (4-(pyridin-4-yl)phenyl)(thianthren-2-yl)methanone (p-TCPy/m-TCPy/o-TCPy):

In a 50 mL round-bottom flask, 4-Pyridinylboronic acid (184 mg, 1.498 mmol), *p*-BrBT (500 mg, 1.249 mmol) and [Pd(PPh3)4] (13.4 mg, 0.0058 mmol), and potassium carbonate (517.8 mg, 3.74 mmol) were introduced under an inert nitrogen atmosphere. A solvent mixture of THF and water in a 3:1 ratio was added to the reaction flask using a syringe. The resulting mixture was thoroughly degassed by performing three successive freeze–pump–thaw cycles to remove dissolved gases and ensure an oxygen-free environment. The reaction mixture was then heated

to reflux and maintained under these conditions for 24 hours, allowing the cross-coupling reaction to proceed to completion. After cooling to room temperature, the reaction mixture was transferred to a separating funnel and extracted with chloroform and water. The combined organic layers were dried over anhydrous sodium sulfate and concentrated under reduced pressure using a rotary evaporator. The crude product obtained was further purified by silica gel column chromatography, using 80% chloroform/hexane mixture eluent system, to afford 375 mg of the desired yellow solid (75.62% yield). ^{1}H NMR (600 MHz, $CDCl_3$) δ 8.75 – 8.71 (m, 1H), 7.93 – 7.87 (m, 2H), 7.79 – 7.74 (m, 1H), 7.70 (dd, *J* = 8.0, 1.8 Hz, 1H), 7.61 – 7.54 (m, 2H), 7.49 (td, *J* = 5.4, 3.3 Hz, 1H), 7.31 – 7.26 (m, 1H). ^{13}C NMR (151 MHz, $CDCl_3$) δ 194.56, 150.51, 147.09, 142.25, 141.41, 137.53, 136.75, 135.97, 134.63, 134.37, 132.15, 132.08, 130.71, 129.92, 129.16, 128.89, 128.79, 128.47, 128.44, 128.18, 128.12, 127.14.

Similarly, *m*-TCPy was synthesized following the same procedure as *p*-TCPy, and a light yellow product is obtained with 65.34 % yield (325 mg). ^{1}H NMR (600 MHz, $CDCl_3$) δ 8.63 – 8.60 (m, 2H), 7.76 (dt, *J* = 7.9, 1.4 Hz, 1H), 7.64 (d, *J* = 2.0 Hz, 1H), 7.55 – 7.50 (m, 2H), 7.42 – 7.38 (m, 4H), 7.38 – 7.36 (m, 1H), 7.35 – 7.30 (m, 2H), 7.23 – 7.19 (m, 2H). ^{13}C NMR (151 MHz, $CDCl_3$) δ 194.79, 150.47, 147.19, 141.53, 138.70, 138.22, 136.66, 136.10, 134.60, 134.32, 132.14, 132.08, 131.01, 130.39, 129.91, 129.26, 129.19, 128.90, 128.78, 128.56, 128.48, 128.43, 128.27, 128.20, 128.13, 121.67.

Similarly, *o*-TCPy was synthesized following the same procedure as *p*-TCPy, and a light yellow product is obtained with 64.53 % yield (320 mg). ^{1}H NMR (600 MHz, $CDCl_3$) δ 8.46 (d, *J* = 5.0 Hz, 2H), 7.77 (s, 1H), 7.64 (t, *J* = 7.5 Hz, 1H), 7.58 – 7.47 (m, 4H), 7.46 – 7.40 (m, 3H), 7.26 (q, *J* = 6.3 Hz, 2H), 7.18 (s, 1H), 1.27 (s, 1H). ^{13}C NMR (151 MHz, $CDCl_3$) δ 196.11, 149.73, 147.86, 142.33, 138.51, 138.23, 136.35, 135.82, 134.35, 134.07, 130.97, 130.05, 129.79, 129.04, 129.02, 128.80, 128.74, 128.45, 128.42, 128.19, 128.12, 123.65.

Synthesis of 2-((4-(pyridin-4-yl)phenyl)(thianthren-2-yl)methylene)malononitrile (p-TPy/m-TPy/o-TPy):

In a dry round-bottom flask, *p*-TCPy (100 mg, 0.2519 mmol) and malononitrile (82.58 mg, 1.25 mmol) were dissolved in dry dichloromethane (DCM) and stirred at 0 °C under an argon atmosphere. To this chilled reaction mixture, titanium tetrachloride ($TiCl_4$) (189.6 mg, 1 mmol) was added dropwise with continuous stirring. The mixture was maintained at 0 °C and stirred for an additional 30 minutes to allow for complete activation. Subsequently, piperidine (468.3 mg, 5 mmol) was added slowly to the reaction mixture, and the temperature was gradually raised to reflux. The reaction was continued under reflux conditions for 4 hours. Upon completion, the reaction mixture was cooled to room temperature and transferred to a separating funnel. The organic phase was extracted using DCM and washed with brine solution to remove any inorganic residues. The combined organic extracts were dried over anhydrous sodium sulfate, filtered, and concentrated under reduced pressure. The resulting crude product was purified by silica gel column chromatography using a 50% ethyl acetate/hexane mixture as the eluent. This afforded 85 mg of the desired yellow solid (75.74 % yield).^{1}H NMR (600 MHz, $CDCl_3$) δ 8.53 (d, *J* = 5.2 Hz, 2H), 7.72 – 7.67 (m, 3H), 7.56 (d, *J* = 8.3 Hz, 2H), 7.50 (dd, *J* = 8.0, 1.8 Hz, 1H), 7.40 (d, *J* = 8.0 Hz, 1H), 7.37 – 7.35 (m, 2H), 7.29 (td, *J* = 5.7, 3.3 Hz, 2H), 7.08 (dd, *J* = 5.8, 3.3 Hz, 2H). ^{13}C NMR (151 MHz, $CDCl_3$) δ 172.28, 150.57, 146.51, 142.61, 142.04, 136.83, 136.02, 135.12, 134.03, 133.98, 131.29, 129.92, 129.36, 128.98, 128.84, 128.82, 128.38, 128.36, 127.64, 121.65, 113.61, 113.48, 82.18. HRMS (ESI) *m*/*z*: $[M + H]^+$ calcd for $C_{27}H_{15}N_3S_2$, 446.0781; found, 446.0782.

Similarly, *m*-TPy was synthesized following the same procedure as *p*-TPy, and a orange product is obtained with 76.63 % yield (86 mg). ^{1}H NMR (600 MHz, $CDCl_3$) δ 8.64 – 8.61 (m, 2H), 7.77 (ddt, *J* = 7.8, 1.9, 1.0 Hz, 1H), 7.65 (d, *J* = 2.0 Hz, 1H), 7.57 – 7.51 (m, 2H), 7.43 – 7.32 (m, 7H), 7.24 – 7.21 (m, 2H). ^{13}C NMR (151 MHz, $CDCl_3$) δ 172.58, 150.57, 146.63, 142.16, 139.40, 136.88, 136.47, 135.00, 134.00, 133.95, 131.35, 130.82, 129.96, 129.83, 129.33, 128.96, 128.83, 128.38, 128.35, 121.74, 113.64, 113.37, 82.60. HRMS (ESI) *m*/*z*: $[M + H]^+$ calcd for $C_{27}H_{15}N_3S_2$, 446.0781; found, 446.0786.

Similarly, *o*-TPy was synthesized following the same procedure as *p*-TPy, and a red solid product is obtained with 70.39 % yield (79 mg). ^{1}H NMR (600 MHz, $CDCl_3$) δ 8.44 (d, *J* = 5.1 Hz, 4H), 7.71 (t, *J* = 7.6 Hz, 2H), 7.64 (t, *J* = 7.6 Hz, 2H), 7.55 (d, *J* = 7.7 Hz, 2H), 7.45 (ddd, *J* = 10.0, 5.5, 2.7 Hz, 7H), 7.36 (d, *J* = 8.0 Hz, 2H), 7.33 – 7.27 (m, 6H), 7.15 (s, 1H), 7.14 (s, 3H), 6.98 (d, *J* = 5.6 Hz, 4H). ^{13}C NMR (151 MHz, $CDCl_3$) δ 173.02, 149.69, 147.10, 142.03, 139.81, 136.49, 134.89, 134.74, 133.84, 133.82, 132.28, 130.74, 130.57, 129.19, 129.08, 128.92, 128.76, 128.63, 128.47, 128.37, 128.32, 123.45, 113.13, 112.92, 84.58. HRMS (ESI) *m*/*z*: $[M + H]^+$ calcd for $C_{27}H_{15}N_3S_2$, 446.0781; found, 446.0779.

Synthesis of 4-(4-(2,2-dicyano-1-(thianthren-2-yl)vinyl)phenyl)-1-methylpyridin-1-ium (p-TPyMe):

In a round-bottom flask, *p*-TPyMe was placed and degassed under an inert atmosphere to remove dissolved gases. Separately, methyl iodide was dissolved in dry acetonitrile. The resulting solution was added to the flask containing p-TPyMe. The reaction mixture was then heated to reflux and maintained under these conditions for 12 hours. Upon completion of the reaction, the excess methyl iodide and acetonitrile were removed by rotary evaporation under reduced pressure. A red solid powder was obtained as the final product, with a quantitative yield (100%).^{1}H NMR (600 MHz, DMSO) δ 9.09 (d, *J* = 6.5 Hz, 1H), 8.61 – 8.57 (m, 1H), 8.26 – 8.22 (m, 1H), 7.83 – 7.74 (m, 2H), 7.66 – 7.53 (m, 3H), 7.48 (dd, *J* = 8.2, 2.0 Hz, 0H), 7.45 – 7.38 (m, 1H). ^{13}C NMR (151 MHz, DMSO) δ 171.22, 153.31, 146.31, 140.46, 138.92, 137.54, 135.87, 135.49, 133.67, 133.65, 132.51, 131.98, 131.92, 131.80, 130.35, 130.07, 129.48, 129.43, 129.27, 129.19, 129.00, 125.20, 114.33, 84.54, 65.39, 47.81, 40.42, 40.28, 40.14, 40.01, 39.87, 39.73, 39.59, 15.64.

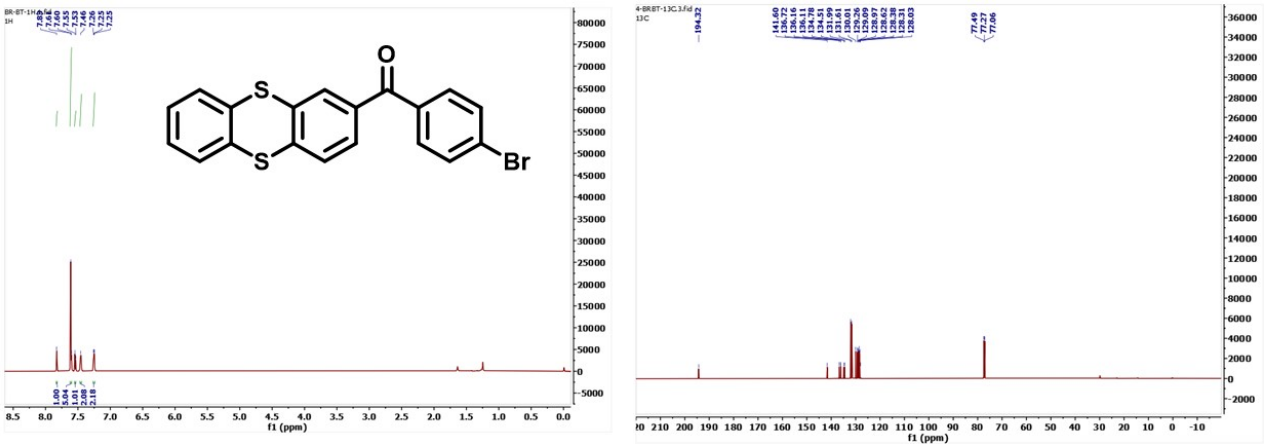

Figure S1. ^{1}H and ^{13}C NMR spectra of *p*-BrBT.

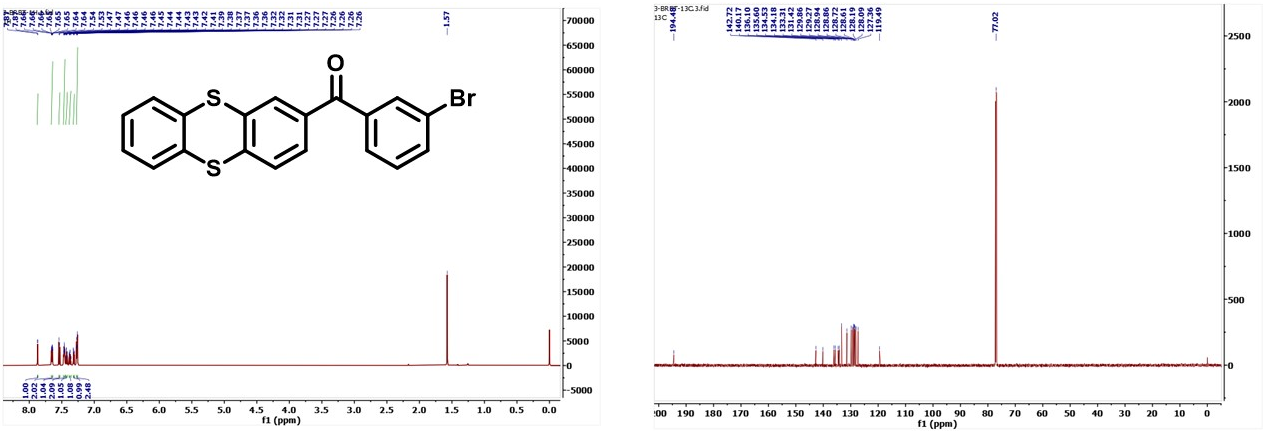

Figure S2. ^{1}H and ^{13}C NMR spectra of *m*-BrBT.

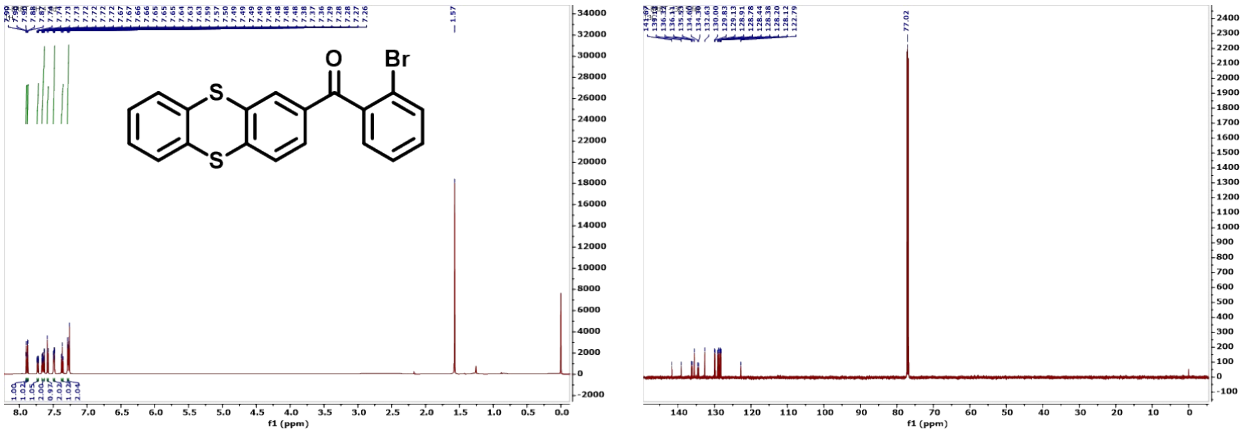

Figure S3. ^{1}H and ^{13}C NMR spectra of *o*-BrBT.

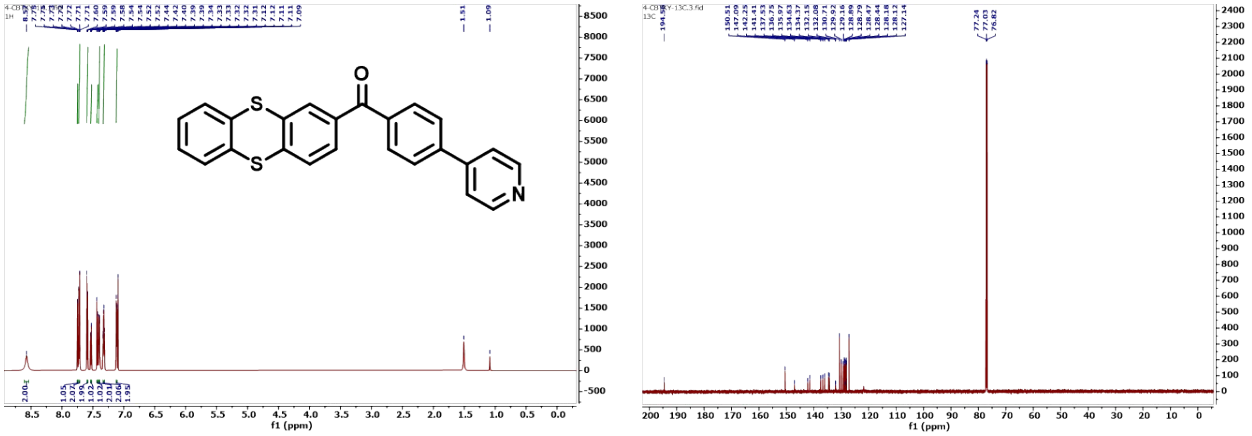

Figure S4. ^{1}H and ^{13}C NMR spectra of *p*-TCPy.

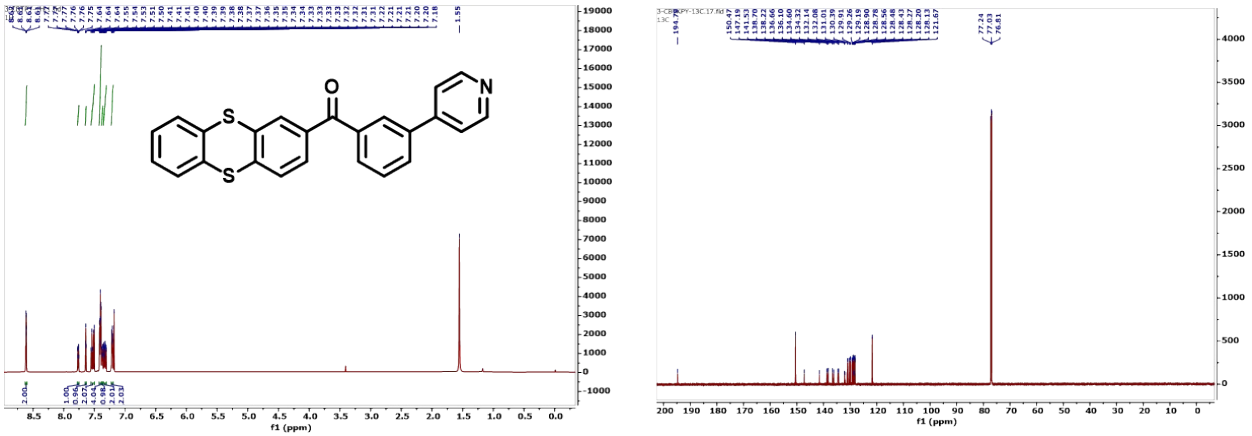

Figure S5. ^{1}H and ^{13}C NMR spectra of *m*-TCPy.

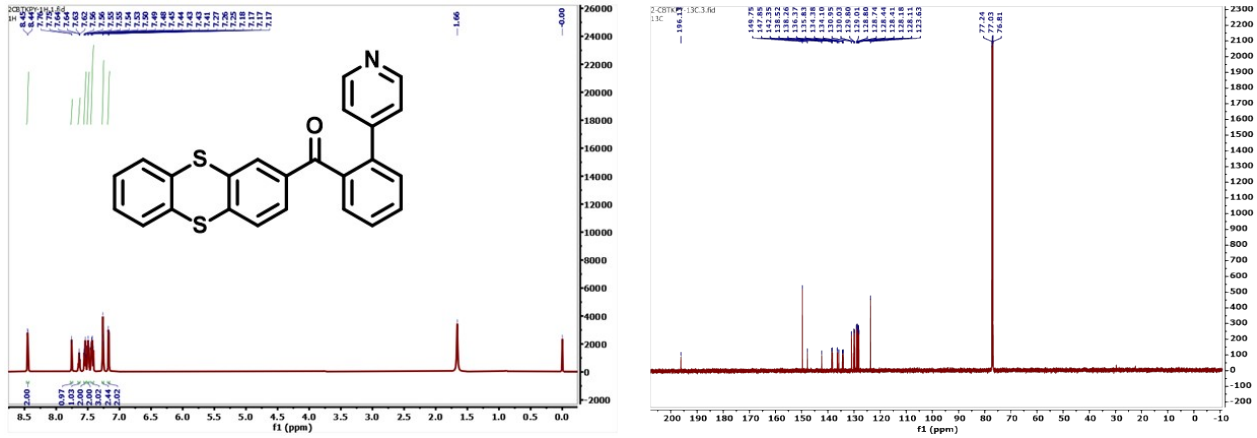

Figure S6. ^{1}H and ^{13}C NMR spectra of *o*-TCPy.

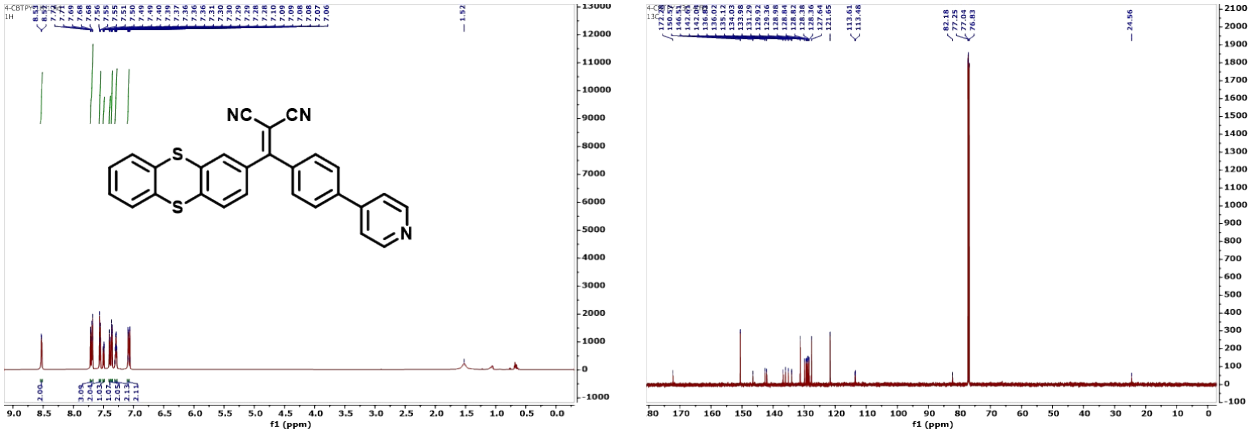

Figure S7. ^{1}H and ^{13}C NMR spectra of *p*-TPy.

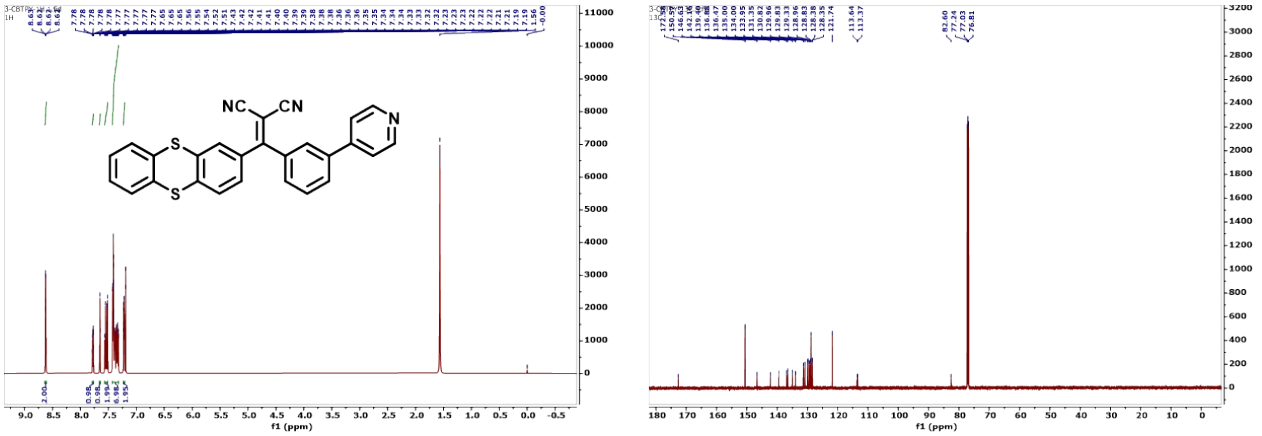

Figure S8. ^{1}H and ^{13}C NMR spectra of *m*-TPy.

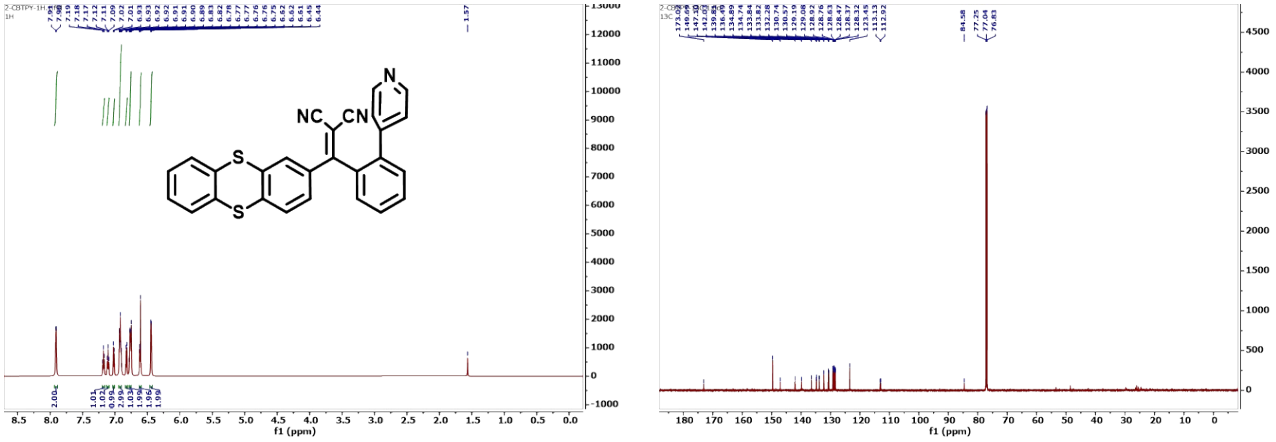

Figure S9. ^{1}H and ^{13}C NMR spectra of *o*-TPy.

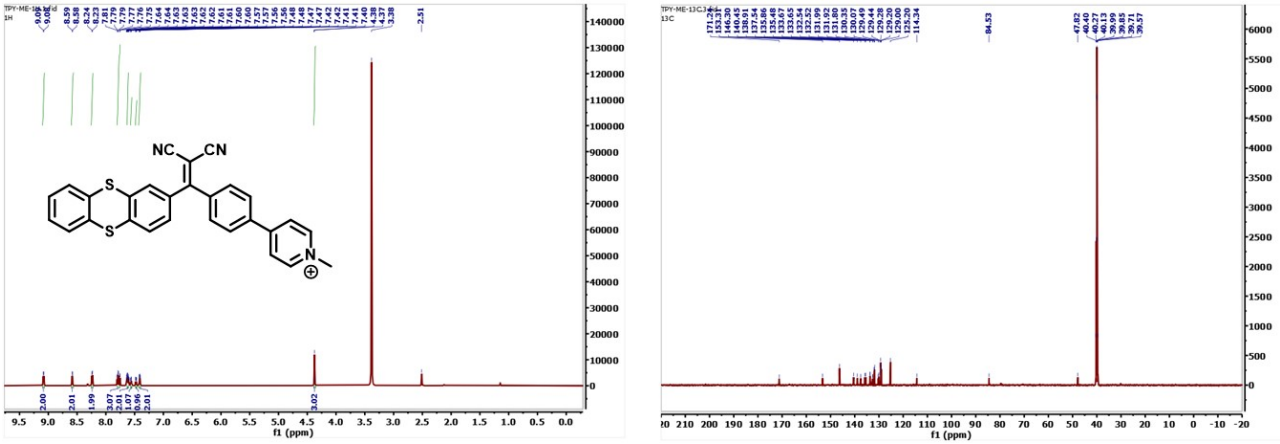

Figure S10. ^{1}H and ^{13}C NMR spectra of *p*-TPyMe.

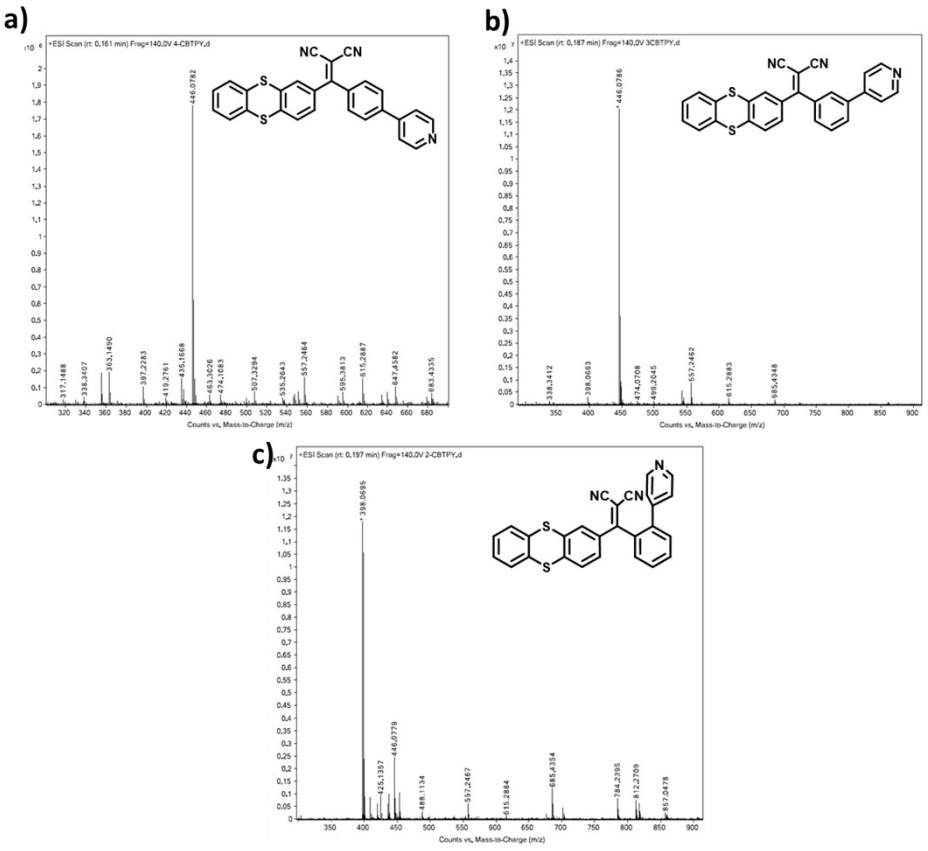

Figure S11. HRMS spectra of a) *p*-TPy, b) *m*-TPy and c) *o*-TPy.

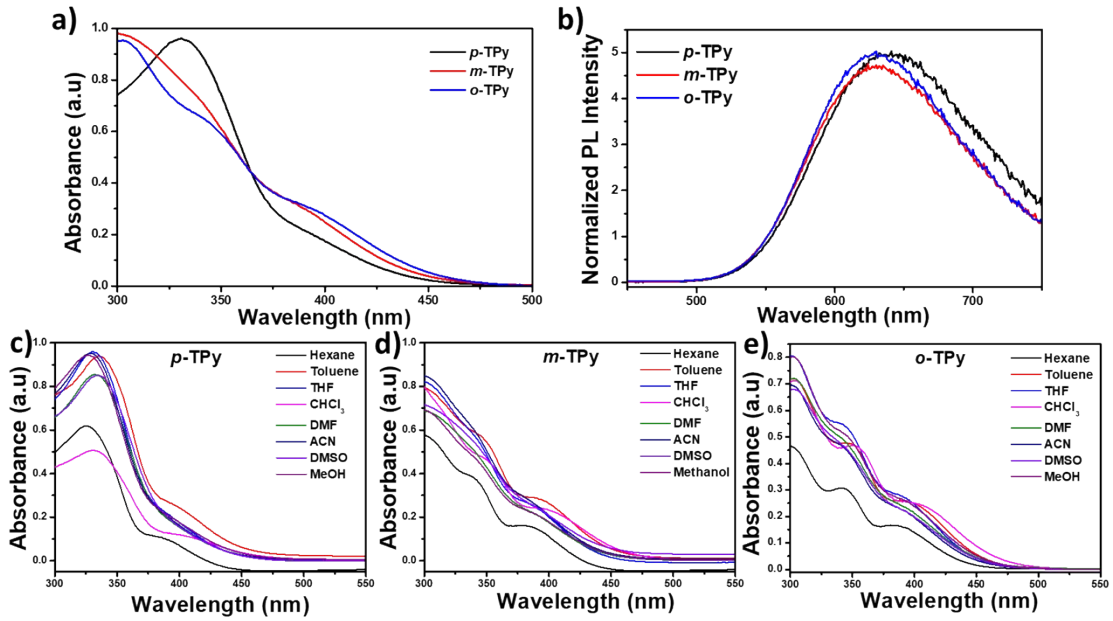

Figure S12. a) Absorption and b) emission spectra of all the positional isomers in solution and aggregated state, respectively (50 µM). Absorption spectra of c) *p*-TPy, d) *m*-TPy and e) *o*-TPy in various solvent polarities.

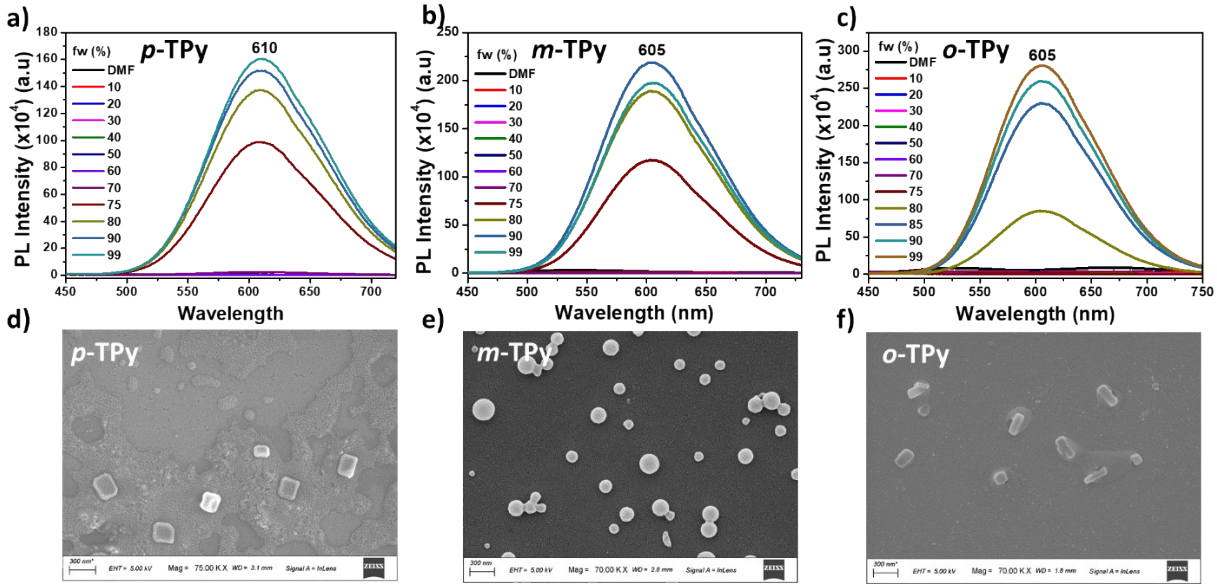

Figure S13. Emission spectra of a) *p*-TPy, b) *m*-TPy and c) *o*-TPy in DMF–water mixtures (0–99% water). FESEM images of nano-aggregates formed by d) *p*-TPy, e) *m*-TPy and f) *o*-TPy upon aggregation in water.

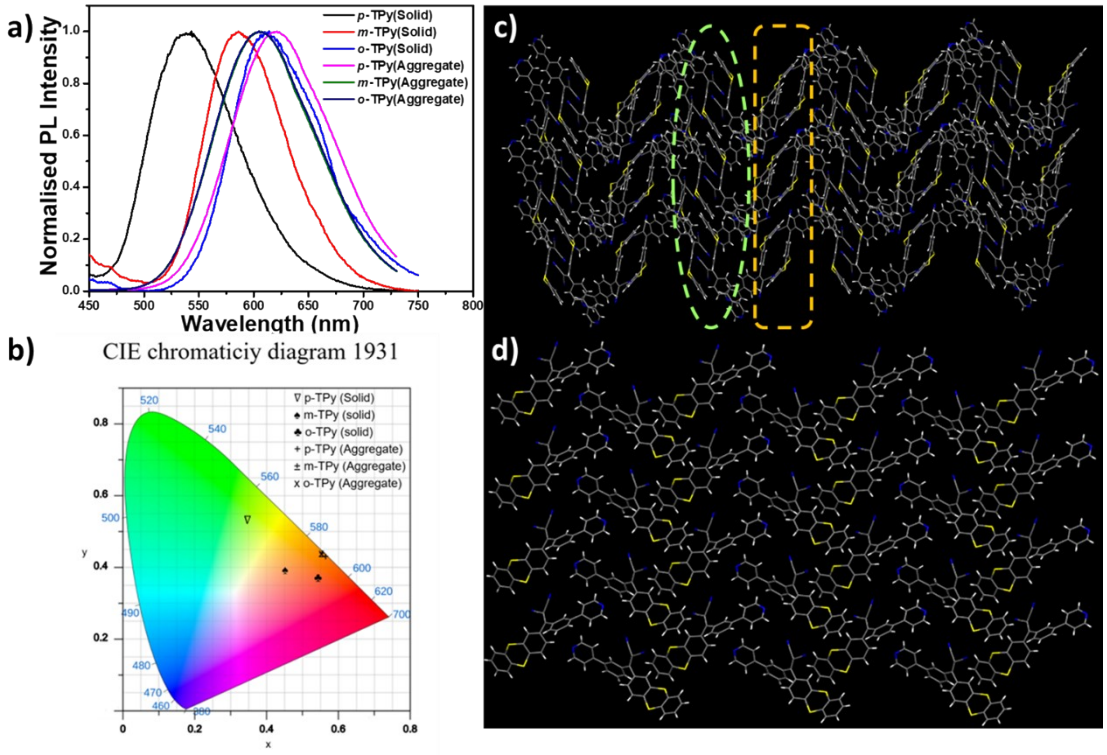

Figure S14. Comparison of the a) emission spectra and b) CIE coordinates of all the isomers in their aggregated and solid state. Bulk packing of c) *p*-TPy and d) *m*-TPy in crystal lattice.

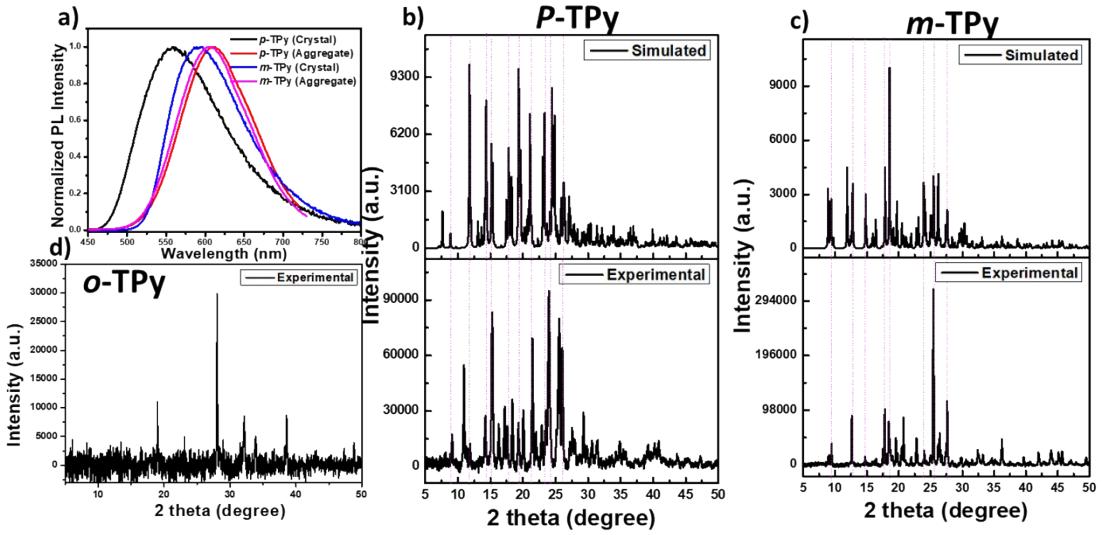

Figure S15. a) Normalized emission spectra of *p*-TPy and *m*-TPy in their crystalline and aggregated state. Comparison of experimental PXRD patterns of all the isomers, b) *p*-TPy, c) *m*-TPy and d) *o*-TPy with their respective simulated PXRD pattern derived from single-crystal X-ray diffraction (SCXRD) data.

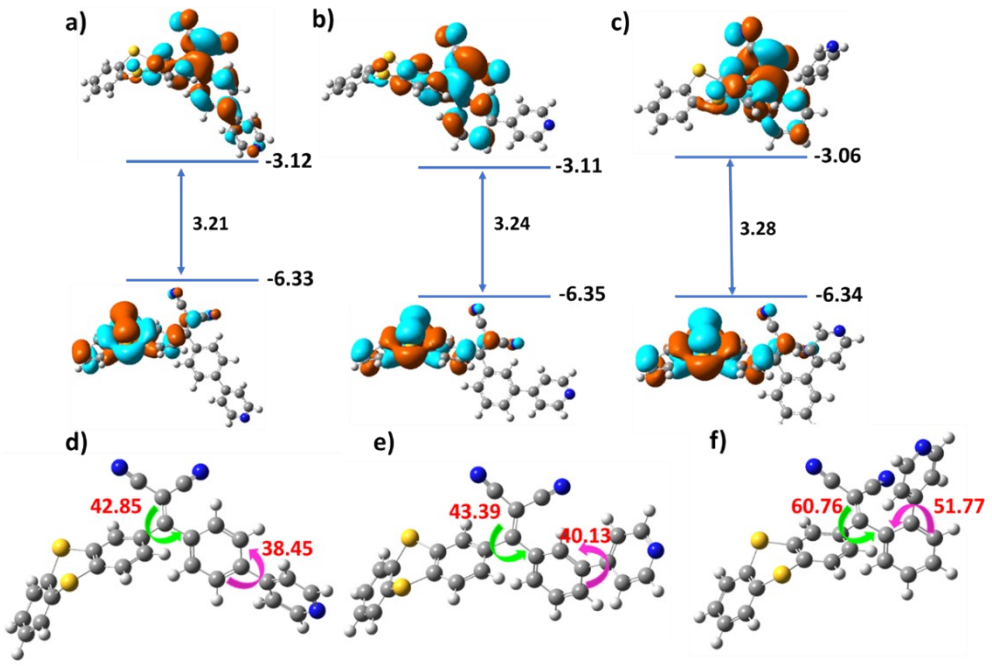

Figure S16. Energy level diagram showing the HOMO and LUMO energy levels of a) *p*-TPy, b) *m*- TPy and c) *o*- TPy as determined at the B3LYP/6-31G(d,p) level. Gaussian optimized molecular structure of d) *p*-TPy, e) *m*- TPy and f) *o*- TPy and their respective dihedral angles.

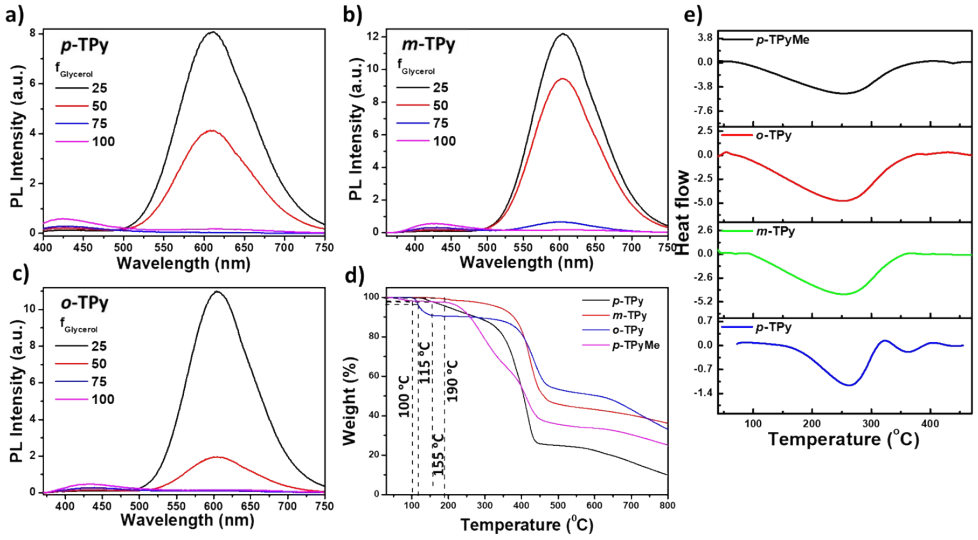

Figure S17. Viscosity dependence study of a) *p*-TPy, b) *m*- TPy and c) *o*- TPy at different water–glycerol mixtures (0–99% glycerol). d) Thermogravimetric analysis (TGA) and e) Differential scanning calorimetry (DSC) measurements of all the luminogens was performed at a heating rate of 10 °C min^{-1} using an alumina crucible under a nitrogen atmosphere.

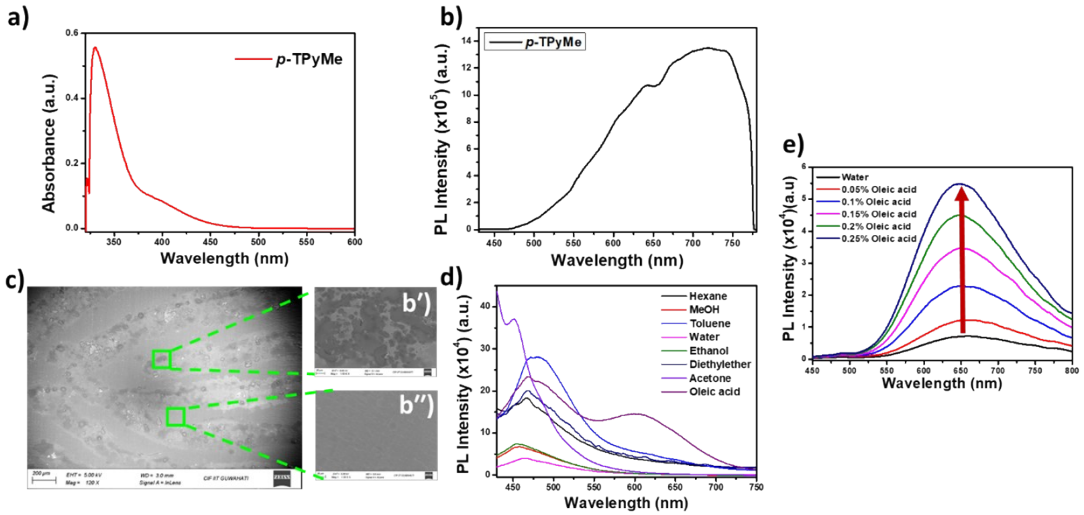

Figure S18. Emission spectra of *p*-TPyMe (50µM) in different acetone/Hexane mixtures. FESEM images of developed latent fingerprints (LFPs) showing preferential adhesion of *p*-TPy to (b′) ridge regions over (b″) furrows, captured at both lower and higher magnifications. d) Emission spectra of *p*-TPyMe in various solvent systems. e) Fluorescence emission spectra of p-TPyMe (50 µM) upon incremental addition of oleic acid (0.05–0.25%).

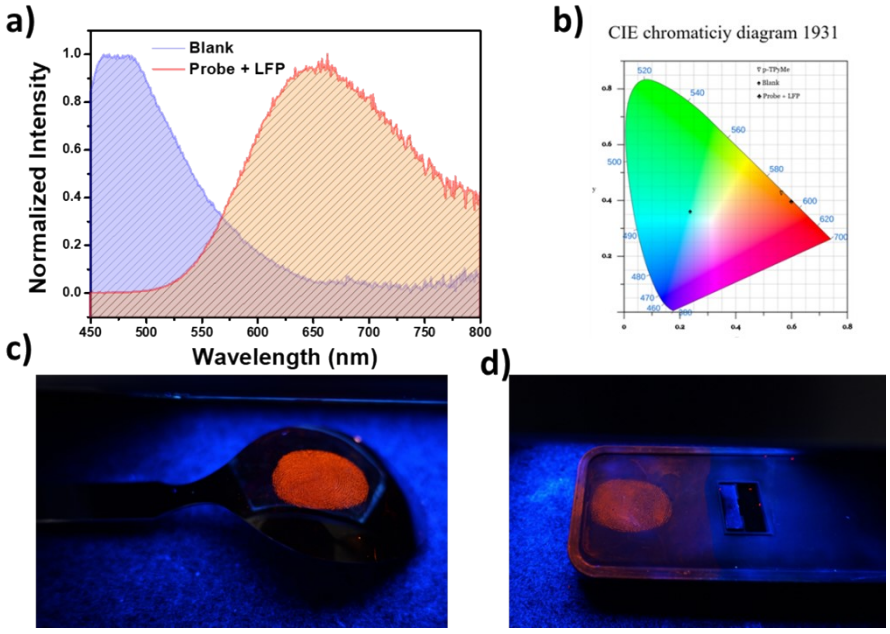

Figure S19. a) Normalized emission spectra of blank substrate and LFP developed with probe (*p*-TPyMe). b) CIE co-ordinates of only the probe (*p*-TPyMe), blank substrate and LFP developed with probe. c) and d) Photographs depicting LFP development on real-life objects such as a spoon and a mobile back cover, respectively.

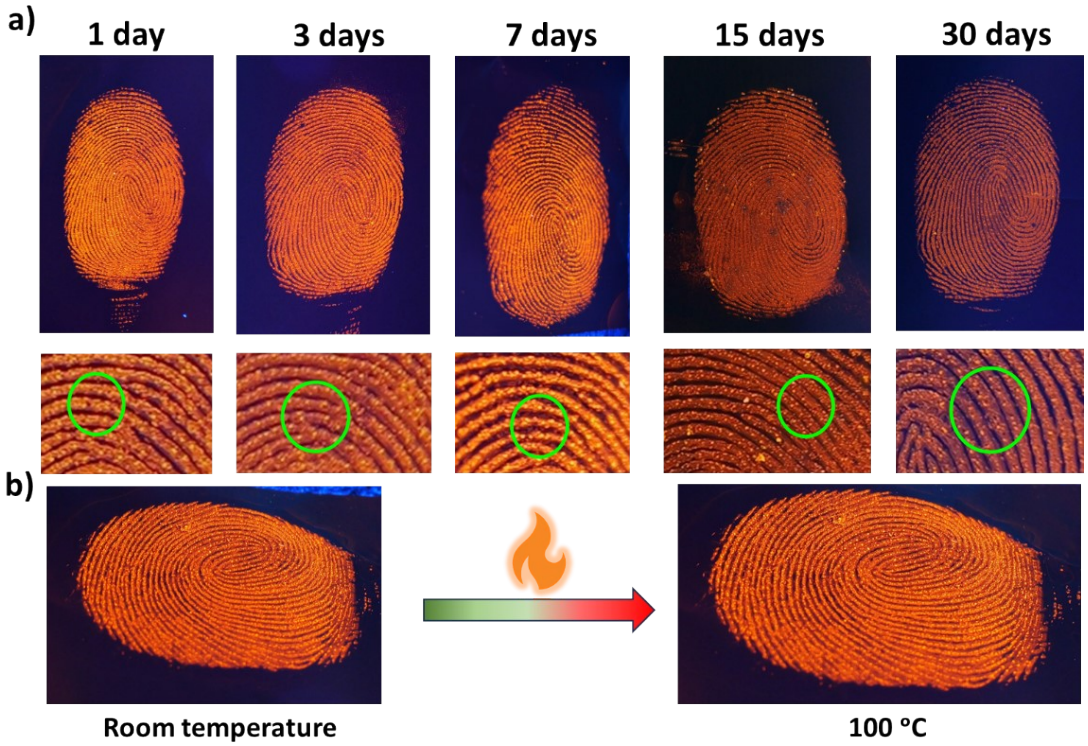

Figure S20. a) The development of LFPs for aged 1, 3, 7, 15 and 30 days with Level 3 details. b) Images of fluorescence thermal stability of the LFP probe.

Table S1. Crystallographic data and structure refinement parameters of *p*-TPy and *m*-TPy.

Compound	***p*-TPy**	***m*-TPy**
Empirical formula	C27 H15 N3 S2	C27 H15 N3 S2
CCDC NO	2451454	2451455
Temperature/K	297(2)	297(2)
Crystal system	monoclinic	monoclinic
Space group	-P 2yn	-P 2yn
a/Å	14.7217(10)	10.8065(11)
b/Å	13.5089(10)	10.2267(10)
c/Å	23.0981(17)	19.839(2)
α/°	90	90
β/°	90.911(2)	90.963(3)
γ/°	90	90
Volume/Å^3	4593.0(6)	2192.2(4)
Z	75	4
ρ_{calc} g/cm^3	1.2886	1.3499
m/mm^{-1}	0.251	0.263
F(000)	1842.5837	921.2918
Index ranges	17 ≤ h ≤ -17 16 ≤ k ≤ -16 27 ≤ l ≤ -27	14 ≤ h ≤ -14 14 ≤ k ≤ -14 27 ≤ l ≤ -27
Reflections used	9316	9709
Data/restraints/parameters	8127/0/576	6107/0/288
Goodness-of-fit on F2	3.0581	1.1354
Final R indexes [I>=2σ (I)]	R1 = 0.1415, wR2 = 0.3968	R1 = 0.0792, wR2 = 0.1495
Final R indexes [all data]	R1 = 0.1194, wR2 = 0.3805	R1 = 0.0590, wR2 = 0.1766